

Surface deformation caused by the Abrikosov vortex lattice

Pavel Lipavský,^{1,2} Klaus Morawetz,^{3,4} Jan Koláček,² and Ernst Helmut Brandt⁵

¹Faculty of Mathematics and Physics, Charles University, Ke Karlovu 3, 12116 Prague 2, Czech Republic

²Institute of Physics, Academy of Sciences, Cukrovarnická 10, 16253 Prague 6, Czech Republic

³Forschungszentrum Rossendorf, Postfach 51 01 19, 01314 Dresden, Germany

⁴Max Planck Institute for the Physics of Complex Systems, Noethnitzer Street 38, 01187 Dresden, Germany

⁵Max Planck Institute for Metals Research, D-70506 Stuttgart, Germany

(Received 1 February 2008; published 15 May 2008)

In superconductors penetrated by Abrikosov vortices, the magnetic pressure and the inhomogeneous condensate density induce a deformation of the ionic lattice. We calculate how this deformation corrugates the surface of a semi-infinite sample. The effect of the surface dipole is included.

DOI: [10.1103/PhysRevB.77.184509](https://doi.org/10.1103/PhysRevB.77.184509)

PACS number(s): 74.20.De, 74.25.Ld, 74.25.Qt, 74.81.-g

I. INTRODUCTION

The deformations of the ionic lattice caused by Abrikosov vortices have been studied from several aspects. For example, if a vortex moves, the motion of such a deformation demands a motion of ions, which contributes to the inertial mass of the vortex.¹⁻³ In the static case, forces evoked by the vortices create a tension, which modifies the total volume of the sample and which is observed as magnetostriction.⁴ Moreover, in anisotropic materials, the elastic energy caused by the vortices depends on the relative orientation of the Abrikosov vortex lattice and the crystal lattice.^{5,6}

In the above mentioned studies, a vortex was treated as infinitely long. This idealized geometry essentially simplifies the problem. Since the system has translational symmetry along the vortex line, the lattice deformation is purely longitudinal, with the displacement vectors perpendicular to the vortex.^{1,4}

As far as we know, nobody has studied deformations near the surface, where the magnetic flux of the vortex leaves the superconductor. In the present paper, we focus on this problem. For simplicity, we assume that the sample is semi-infinite and the applied magnetic field is perpendicular to its surface; see Fig. 1.

Far from the surface, the lattice deformation approaches its bulk value with displacement vectors perpendicular to vortices, i.e., parallel to the surface. Let us sketch in advance which complications one can expect near the surface.

As seen in Fig. 1, the stretching magnetic field, together with the circulating currents, results in a Lorentz force with a component pointing along the vortex. The electric fields balancing this force also act on the ion lattice and corrugate the surface.

Beside the Lorentz force, one can imagine two additional mechanisms leading to the corrugation. First, the specific volume of the superconducting and normal states differ. The normal metal in the vortex core is pulled by its neighbor to adopt the specific volume of the superconductor. As mentioned above, deep in the bulk, these stresses cause displacements perpendicular to the vortex. Close to the surface, however, the same stresses lead to different deformations as they are partially relaxed by displacements perpendicular to the surface, i.e., along the vortex.

Second, the surface dipole that confines the electrons in the crystal changes in transition from the normal to the superconducting state. Accordingly, at the vortex core, the surface dipole differs from the other regions of the surface. The force that holds the electrons inward naturally pulls the oppositely charged ions outward and also corrugates the surface. The general relation between the surface dipole and the surface tension was already established two decades ago.^{7,8} Only recently, the contribution of the superconducting condensate was discussed.⁹

The paper is organized as follows: In Secs. II and III, we introduce the basic set of equations for elastic deformations of an isotropic material near the surface. The surface deformation due to the Abrikosov vortex lattices is discussed in Sec. IV and the numerical solutions for Nb and YBa₂Cu₃O₇ are presented in Sec. V. Section VI, with the conclusions, ends the paper.

II. ELASTIC DEFORMATIONS IN ISOTROPIC MEDIUM

In this section, we recall the basic definitions needed to describe the elastic deformations of an isotropic medium. There are more details in which the reader can find in the textbook of Landau and Lifshitz.¹⁰

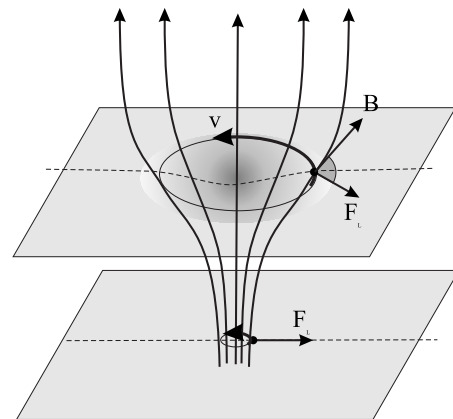


FIG. 1. Lorentz force acting on the circulating superconducting current. In the bulk, the Lorentz force is parallel to the surface. Near the surface, it is not parallel due to the magnetic stray field.

A. Tensors of strain and stress

The deformations are described by atomic displacements \mathbf{u} . We assume that all atoms are identical and only a single atom occupies the elementary cell. Since the interatomic distance is short compared to the characteristic scales of deformations, we treat $\mathbf{u}(x, y, z)$ as a function of continuous coordinates.

The space derivatives of the displacement define the strain tensor. For small deformations assumed here, its components read as

$$u_{xy} = \frac{1}{2} \left(\frac{\partial u_x}{\partial y} + \frac{\partial u_y}{\partial x} \right). \quad (1)$$

The complementary antisymmetric combination of the derivatives corresponds to the rotation of the rigid body; therefore, it does not contribute to deformations.

The strain creates a stress described by a tensor σ . In general $\sigma_{\kappa\tau} = \sum_{\mu\nu} \Lambda_{\kappa\tau\mu\nu} \mu_{\mu\nu}$, where Λ is the fourth order tensor of the elastic coefficients. The Greek indices stand for x, y, z . For an isotropic medium, this relation simplifies to

$$\sigma_{\kappa\tau} = K(\nabla \cdot \mathbf{u}) \delta_{\kappa\tau} + 2\mu \left[u_{\kappa\tau} - \frac{1}{3}(\nabla \cdot \mathbf{u}) \delta_{\kappa\tau} \right], \quad (2)$$

where the divergence of the displacement vector

$$(\nabla \cdot \mathbf{u}) = u_{xx} + u_{yy} + u_{zz} \quad (3)$$

is a shorthand notation for the trace of the strain tensor. It represents the local change in the specific volume. The tensor $u_{\kappa\tau} - 1/3(\nabla \cdot \mathbf{u}) \delta_{\kappa\tau}$ has zero trace and purely describes the shear deformations. The coefficients K and μ are called the bulk and shear moduli, respectively.

B. Stability conditions

The stress depends on the local gradients of the displacements, i.e., on the changes in the bond lengths between neighboring atoms. Accordingly, it only represents contact forces while long-range forces have to be separately covered. Here, we shall consider a noncontact force that is due to the interaction of the crystal lattice with superconducting electrons.

The gradient of the stress balances a long-range force \mathbf{F} acting on a unitary volume $\sum_{\kappa} \nabla_{\kappa} \sigma_{\kappa\tau} + F_{\tau} = 0$, where $\nabla_x \equiv \partial / \partial x$ and so on. For the isotropic material, this stability condition reads as¹⁰

$$\left(K + \frac{4}{3}\mu \right) \nabla (\nabla \cdot \mathbf{u}) - \mu [\nabla \times (\nabla \times \mathbf{u})] = \mathbf{F}. \quad (4)$$

In this paper, we consider forces that can be expressed as a gradient of the potential U ,

$$\mathbf{F} = -\nabla U. \quad (5)$$

In our numerical studies below, we assume that this potential is exclusively due to the electrostatic potential φ acting on the charge density of the ionic lattice ρ , i.e., $U = \rho\varphi$.

Alternatively, one can assume an effective potential $U = 2K\alpha_0|\psi|^2/n$, which corresponds to the force used by

Šimánek and Duan^{1,2} and Coffey.⁴ Here, α_0 is the relative volume difference between the superconducting and the normal states, K is the bulk modulus, ψ is the Ginzburg–Landau (GL) wave function, and n is the density of pairable electrons.

These two choices of the potential U yield very similar results. They are not completely identical, however. For example, the electrostatic potential known as the Bernoulli potential covers the Lorentz force, while the effective potential $U = 2K\alpha_0|\psi|^2/n$ does not.¹¹

C. Surface conditions

At the surface, the balance of forces demands the $\sum_{\kappa} n_{\kappa} \sigma_{\kappa\tau} + P_{\tau} = 0$, where \mathbf{n} is a unit vector that is normal to the surface and \mathbf{P} is the external force on a unit area of the surface. The normal component $p = (\mathbf{n} \cdot \mathbf{P})$ is the pressure. We will not assume tangential surface forces in this paper.

To simplify boundary conditions, we specify the geometry of our sample. It is a semi-infinite superconductor in the half-space $z > 0$. For the normal vector $\mathbf{n} = (0, 0, -1)$ and normal surface force $\mathbf{P} = (0, 0, -p)$, we find three surface conditions,

$$\begin{pmatrix} \sigma_{xz} \\ \sigma_{yz} \\ \sigma_{zz} \end{pmatrix} = \begin{pmatrix} 0 \\ 0 \\ -p \end{pmatrix}. \quad (6)$$

By using the linear relation between stress and strain, the surface conditions [Eq. (6)] are converted into the conditions of the displacement \mathbf{u} . For the isotropic medium from Eqs. (2) and (6) follows

$$u_{xz} = 0,$$

$$u_{yz} = 0,$$

$$\left(K + \frac{4}{3}\mu \right) u_{zz} + \left(K - \frac{2}{3}\mu \right) (u_{xx} + u_{yy}) = -p. \quad (7)$$

The pressure p includes the ambient pressure of the coolant, which is homogeneous all over the sample surface. We ignore it because it does not contribute to the corrugation.

We do not want to list all possible forces acting on the surface. We merely mention that the surface of the sample feels the surface dipole $\delta\varphi$, which acts as an effective pressure $p = -\rho\delta\varphi$; see Ref. 9. The dipole amplitude $\delta\varphi = \varphi(0) - \varphi(\infty)$ is the difference between the electrostatic potentials at the surface and deep in the bulk of the superconductor. The surface dipole is conveniently evaluated from the GL free energy with the help of the Budd–Vannimenus theorem^{12,13} adopted to the case of a superconductor.^{9,14}

Now the problem is fully specified. The displacement \mathbf{u} is driven by the potential U and the effective pressure p . These quantities can be treated within any approximation the reader prefers. In Sec. V, we will relate them to the electrostatic potential φ and the surface dipole $\delta\varphi$. At the moment, we merely assume that the potential and the pressure are known functions of the GL wave function. Since the deformation has only a negligible effect on GL wave function, the GL

wave function obtained from the ordinary GL theory can be used. We take the GL wave function as known and focus on the deformation.

III. INDUCED AND FREE DEFORMATION

As mentioned in Sec. I, the deformation near the surface has three sources: magnetic stray field, expansion or contraction along the vortex, and the surface dipole. Since elastic equation (4) and its boundary conditions [Eq. (7)] are linear in \mathbf{u} , it is possible to separate individual contributions.

As the first step, it is advantageous to separate the displacement \mathbf{u} into two parts: the induced deformation \mathbf{u}^i driven by the long range force \mathbf{F} , which induces displacements all over the sample, and the free deformation \mathbf{u}^f . So we write

$$\mathbf{u} = \mathbf{u}^i + \mathbf{u}^f, \quad (8)$$

where the displacement \mathbf{u}^i is longitudinal,

$$[\nabla \times \mathbf{u}^i] = 0, \quad (9)$$

and obeys the equation

$$\left(K + \frac{4}{3}\mu\right)(\nabla \cdot \mathbf{u}^i) = -U(\mathbf{r}, z). \quad (10)$$

Since differential equation (10) is of the first order, this induced displacement is fully specified by the potential U and the requirement of the convergence deep in the sample.

After substitution of Eq. (8) into elastic equation (4), the stress from the induced displacement compensates for the long-range forces and one is left with the equation for free displacement,

$$\left(K + \frac{4}{3}\mu\right) \nabla (\nabla \cdot \mathbf{u}^f) - \mu[\nabla \times (\nabla \times \mathbf{u}^f)] = 0. \quad (11)$$

This is a second-order differential equation and we need to find the solution, which in addition to the convergence deep inside, also guarantees the fulfillment of the surface boundary condition.

A. Laplace equation for free deformation

Now we show that it is possible to simplify Eq. (11) to the Laplace equation. By taking the divergence of Eq. (11), we find that

$$\nabla \cdot (\nabla^2 \mathbf{u}^f) = 0 \quad (12)$$

because the divergence of a rotation is zero. By taking the rotation of Eq. (11), we find that

$$[\nabla \times (\nabla^2 \mathbf{u}^f)] = 0 \quad (13)$$

because the rotation of a gradient is also zero. The vector identity $[\nabla \times (\nabla \times \mathbf{u}^f)] = \nabla(\nabla \cdot \mathbf{u}^f) - \nabla^2 \mathbf{u}^f$ was used in the rearrangement.

According to Eqs. (12) and (13), all of the derivatives of $\nabla^2 \mathbf{u}^f$ are zero; therefore, it is constant. A finite value of \mathbf{u}^f for $z \rightarrow \infty$ is possible only if this constant is zero. Thus, we have

$$\nabla^2 \mathbf{u}^f = 0. \quad (14)$$

Being free of material parameters, the Laplace equation is more convenient than Eq. (11).

B. Surface matching

Surface boundary condition (7) applies to the total displacement. By substituting Eq. (8) into Eq. (7), we obtain

$$u_{xz}^f = -u_{xz}^i,$$

$$u_{yz}^f = -u_{yz}^i,$$

$$\begin{aligned} & \left(K + \frac{4}{3}\mu\right)u_{zz}^f + \left(K - \frac{2}{3}\mu\right)(u_{xx}^f + u_{yy}^f) \\ & = -p - \left(K + \frac{4}{3}\mu\right)u_{zz}^i - \left(K - \frac{2}{3}\mu\right)(u_{xx}^i + u_{yy}^i). \end{aligned} \quad (15)$$

These conditions determine the gradients of \mathbf{u}^f at $z=0$. The induced deformation \mathbf{u}^i is already known; therefore, we have moved its strain elements to the right hand side of the boundary conditions.

By boundary conditions (15), the free displacement is fully specified. The second boundary condition is the request of convergence, $u^f \rightarrow 0$ for $z \rightarrow \infty$. Now, the set of equations is complete and we are ready to solve for the corrugation of the surface around the vortex ends.

IV. VORTEX LATTICE

If the vortices form an Abrikosov lattice, we can benefit from its periodic structure. In this case, all components of the displacement can be analytically solved in the two-dimensional (2D) Fourier representation.

A. Induced deformation

In the x - y plane, the potential is a sum of planar waves,

$$U(\mathbf{r}, z) = \sum_k e^{i\mathbf{k}\mathbf{r}} U(\mathbf{k}, z), \quad (16)$$

where $\mathbf{r} \equiv (x, y)$ is a 2D coordinate. The 2D wave vectors $\mathbf{k} = (k_x, k_y)$ attain discrete values given by the density of vortices and the actual structure of the Abrikosov lattice.

To solve the equation for the displacement, some intermediate steps are required. Since the induced displacement \mathbf{u}^i is longitudinal, it can be expressed as the gradient of a scalar function,

$$\mathbf{u}^i = \nabla \chi(\mathbf{r}, z). \quad (17)$$

In the 2D Fourier representation, Eq. (10) yields

$$\left(K + \frac{4}{3}\mu\right) \left(k^2 - \frac{\partial^2}{\partial z^2}\right) \chi = U(\mathbf{k}, z), \quad (18)$$

where $k^2 = k_x^2 + k_y^2$. It is solved by

$$\chi(\mathbf{k}, z) = \frac{1}{2k} \frac{1}{K + \frac{4}{3}\mu} \int_0^\infty dz' e^{-k|z-z'|} U(\mathbf{k}, z'). \quad (19)$$

We are interested, namely, in values at the surface,

$$\chi(\mathbf{k}, 0) = \frac{1}{2k} \frac{1}{K + \frac{4}{3}\mu} \int_0^\infty dz' e^{-kz'} U(\mathbf{k}, z'). \quad (20)$$

The z gradient at the surface follows from Eq. (19) as

$$u_z^i = \left. \frac{\partial}{\partial z} \chi(\mathbf{k}, z) \right|_{z=0} = k\chi(\mathbf{k}, 0). \quad (21)$$

The surface value of this displacement contributes to the surface corrugation.

The surface strain given by the second gradient follows from Eq. (18) as

$$u_{zz}^i = \left. \frac{\partial^2}{\partial z^2} \chi(\mathbf{k}, z) \right|_{z=0} = k^2 \chi(\mathbf{k}, 0) - \frac{1}{K + \frac{4}{3}\mu} U(\mathbf{k}, 0). \quad (22)$$

This surface strain enters the boundary condition, wherein it serves as the source of the free deformation.

B. Free deformation

The free deviation \mathbf{u}^f has the same periodicity as that of the Abrikosov vortex lattice. From the Laplace equation (14), thus follows:

$$\mathbf{u}^f(\mathbf{k}, z) = \mathbf{u}^f(\mathbf{k}, 0) e^{-kz}. \quad (23)$$

Boundary conditions (15) in the 2D Fourier representation read as

$$\begin{aligned} \frac{1}{2}(ik_x u_z^f - k u_x^f) &= -ik_x k \chi(\mathbf{k}, 0), \\ \frac{1}{2}(ik_y u_z^f - k u_y^f) &= -ik_y k \chi(\mathbf{k}, 0), \\ -k \left(K + \frac{4}{3}\mu \right) u_z^f + \left(K - \frac{2}{3}\mu \right) (ik_x u_x^f + ik_y u_y^f) \\ &= -p - 2\mu k^2 \chi(\mathbf{k}, 0) + U(\mathbf{k}, 0). \end{aligned} \quad (24)$$

We have used Eq. (23) to evaluate the derivatives on the left hand side of Eq. (15) and ansatz (17) together with relations (20)–(22) in the right hand side of Eq. (15).

From the first and second conditions of Eq. (24), one eliminates u_x^f and u_y^f by obtaining $ik_x u_x^f + ik_y u_y^f = -k u_z^f - 2k^2 \chi$. By using this relation in the third condition of Eq. (24), one arrives at the z component of free displacement,

$$u_z^f = \frac{p - U(\mathbf{k}, 0) - 2k^2 \left(K - \frac{5}{3}\mu \right) \chi(\mathbf{k}, 0)}{2k \left(K + \frac{1}{3}\mu \right)}. \quad (25)$$

With u_z^f from Eq. (25) and the first and the second equations of Eq. (24), one readily evaluates the parallel displacements u_x^f and u_y^f , respectively. Here, we want to concentrate on the component u_z^f perpendicular to the surface.

C. Surface corrugation

The corrugation of the surface is given by the total displacement in the z direction $u_z = u_z^f + u_z^i$. By adding Eqs. (25) and (21), we obtain

$$u_z(\mathbf{k}) = \frac{p - U(\mathbf{k}, 0) + 4k^2 \mu \chi(\mathbf{k}, 0)}{2k \left(K + \frac{1}{3}\mu \right)},$$

$$u_z(\mathbf{r}) = \sum_{\mathbf{k}} e^{i\mathbf{k}\mathbf{r}} u_z(\mathbf{k}). \quad (26)$$

Formula (26) is the final result of the general part of our discussion. It provides the 2D Fourier decomposition of atomic displacements at the surface layer. In our notation, a positive displacement u_z corresponds to the atomic motion inward the superconductor.

V. NUMERICAL RESULTS FOR THE ELECTROSTATIC INTERACTION

To proceed, we assume that the interaction between the superelectrons and the ionic lattice is exclusively carried by the mean electrostatic field. This approximation neglects the effect of the lattice density on the electronic band structure and on the phonon band structure, and for many materials it might lead to quantitatively incorrect predictions. In this paper, we adopt this approximation for its simplicity.

A. Surface dipole

As mentioned in Sec. I, within the electrostatic approximation, the effective potential is proportional to the electrostatic Bernoulli potential φ , i.e.,

$$U(\mathbf{r}, z) = \rho \varphi(\mathbf{r}, z). \quad (27)$$

The Bernoulli potential is a function of the GL function¹⁵

$$e\varphi = -\frac{\partial \alpha}{\partial n} |\psi|^2 - \frac{1}{2} \frac{\partial \beta}{\partial n} |\psi|^4, \quad (28)$$

where $\alpha = \gamma(T^2 - T_c^2)/2n$ and $\beta = \gamma T^2/2n^2$ are the GL parameters expressed in terms of Sommerfeld's gamma. These values follow from the Gorter–Casimir two-fluid model in the limit $T \rightarrow T_c$; see Ref. 16. One can also use the limiting BCS values of α and β , which are larger by factors 1.43 and 2.86 than the two-fluid limit.⁹

The pressure at the surface is caused by the surface dipole⁹

$$p(\mathbf{r}) = \rho \varphi_+(\mathbf{r}) - \rho \varphi_-(\mathbf{r}), \quad (29)$$

where $\varphi_\pm(\mathbf{r}) = \varphi(\mathbf{r}, \pm \epsilon)$, with $\epsilon > 0$ being an infinitesimal distance. In reality, ϵ has to exceed the Thomas–Fermi screening length and the BCS coherence length. The potential φ_+ is the extrapolation of the internal potential toward the surface, and φ_- represents the potential out of the crystal.

The surface value of the effective potential is defined as a limit from inside; therefore,

$$U(\mathbf{r}, 0) \equiv \lim_{\epsilon \rightarrow 0} U(\mathbf{r}, \epsilon) = \rho \varphi_+(\mathbf{r}). \quad (30)$$

The displacement of the surface atoms [Eq. (26)] for the electrostatic approximation reads as

$$u_z = -\frac{\rho}{2k \left(K + \frac{1}{3}\mu \right)} \varphi_-(\mathbf{k}) + \frac{2k\mu}{K + \frac{1}{3}\mu} \chi(\mathbf{k}, 0). \quad (31)$$

TABLE I. Material parameters of niobium and $\text{YBa}_2\text{Cu}_3\text{O}_7$: condensation energy per particle, GL parameter, particle density, logarithmic derivatives of the critical temperature and the linear coefficient of the specific heat γ , Young's modulus, and Poisson ratio.

	$\frac{\gamma T_c^2}{4n}$ (μeV)	κ	n (10^{28} m^{-3})	$\frac{\partial \ln T_c}{\partial \ln n}$	$\frac{\partial \ln \gamma}{\partial \ln n}$	E (GPa)	σ
Nb	4.085	1.5	2.2	0.74 ^a	0.42 ^a	105 ^b	0.4 ^b
YBCO	750	65	0.5	-4.82 ^c	-4.13 ^c	200 ^{d,e}	0.2 ^c

^aReference 16.

^bReference 19.

^cReference 20.

^dReference 21.

^eReference 22.

As one can see, the potential φ_+ cancels and we are left with the potential φ_- . According to the Budd–Vannimenus theorem for superconductors, the potential above the surface is proportional to the density of the free energy,^{14,17}

$$e\varphi_- = -\frac{\alpha}{n}|\psi|^2 - \frac{1}{2} \frac{\beta}{n} |\psi|^4, \quad (32)$$

which one conveniently evaluates within the Ginzburg–Landau theory. For details of the Bernoulli potential and the surface dipole, see Ref. 16.

B. Bulk forces

The internal value of the Bernoulli potential contributes only via the subsidiary function χ . In general, one needs the complete three-dimensional solution of the vortex lattice near the surface. Numerical studies have shown that one can neglect the z dependence of the amplitude of the GL function everywhere, including the close vicinity of the surface.¹⁸ The amplitude variation is about 1%. Since the Bernoulli potential exclusively depends on the amplitude of the GL function, the potential has the same value as deep in the bulk, $\varphi(\mathbf{r}, z) \approx \varphi_\infty(\mathbf{r})$, for any z .

If we neglect the z dependence of the potential, the integral in Eq. (20) becomes trivial, giving

$$\chi(\mathbf{k}, 0) = \frac{1}{2k^2} \frac{\rho}{K + \frac{4}{3}\mu} \varphi_\infty(\mathbf{k}). \quad (33)$$

The potential φ_∞ is conveniently found from Eq. (28) by using the GL function deep in the sample. For a fixed magnetic field, the GL function deep in the sample is the same as that in the infinite sample; therefore, it can be evaluated as an effectively two-dimensional problem.

C. Surface corrugation

The displacement of the surface atoms results from Eqs. (31) and (33) as

$$u_z = -\frac{\rho}{2k(K + \frac{1}{3}\mu)} \left[\varphi_-(\mathbf{k}) - \frac{2\mu}{K + \frac{4}{3}\mu} \varphi_\infty(\mathbf{k}) \right]. \quad (34)$$

One can see from Eq. (34) that the relative contribution of the bulk and the surface potentials depend on the shear modulus μ . For soft materials with $\mu \ll K$, the bulk potential

gives a negligible contribution, so that the surface corrugation is driven only by the electrostatic potential above the surface. In this case, the corrugation is independent of the density derivatives of the GL parameters.

Many authors who deal with deformable superconductors prefer to express elastic coefficients via the Poisson ratio $\sigma = (K - 2/3\mu)/(2K + 2/3\mu)$ and the Young modulus $E = 3K(1 - 2\sigma)$. In this notation, the displacement of surface atoms [Eq. (34)] reads,

$$u_z = \frac{(1 - 2\sigma)(1 + \sigma)}{kE(1 - \sigma)} \{ (1 - \sigma)p(\mathbf{k}) - \rho\sigma\varphi_\infty(\mathbf{k}) \}. \quad (35)$$

By deriving Eq. (35), we have shown that the Bernoulli potential is nearly independent of z , so that $\varphi_+ = \varphi_\infty$. The pressure at the surface [Eq. (29)], thus, equals $p = \rho(\varphi_\infty - \varphi_-)$.

The numerical study of the surface corrugation [Eq. (35)] is performed with the parameters listed in Table I. Figure 2 presents the surface corrugation of niobium with the GL parameters κ that are increased by impurities to 1.5. The scale is in $\text{pm} = 10^{-2} \text{ \AA}$; therefore, the maximum deformation of $\sim 5 \times 10^{-4} \text{ \AA}$ is far too small to be detected by recent scanning microscopes. In our convention, the negative u_z corresponds to the atoms displaced out of the crystal.

The total deviation of the atoms at the surface is seen in the upper part of Fig. 2. The middle part shows the deviation evaluated by omitting the surface dipole, i.e., setting $p=0$ in formula (35). As one can see, such an approximation for niobium leads to the opposite sign of the atomic displacement. The lower part shows the surface deformation evaluated from the surface dipole only. This approximation overestimates the amplitude more than twice.

The magnitude of the surface corrugation is directly proportional to the condensation energy per particle, which for niobium has the value $\frac{\gamma T_c^2}{4n} = 4.6 \mu\text{eV}$. In conventional superconductors, this condensation energy per particle is small because of the small critical temperature, $T_c = 9.5 \text{ K}$, and the large density of particles, $n = 2.2 \times 10^{28}/\text{m}^3$.

In high- T_c superconductors, the critical temperature is higher by a factor of 10, while the density of particles is lower by a factor of 10. This leads to an appreciably larger condensation energy per particle. For example, in $\text{YBa}_2\text{Cu}_3\text{O}_7$, one has $T_c = 90 \text{ K}$ and $n = 5 \times 10^{27} \text{ m}^{-3}$, resulting in $\frac{\gamma T_c^2}{4n} = 750 \mu\text{eV}$. Figure 3 presents a corrugation of the $\text{YBa}_2\text{Cu}_3\text{O}_7$ surface with the surface parallel to the a - b

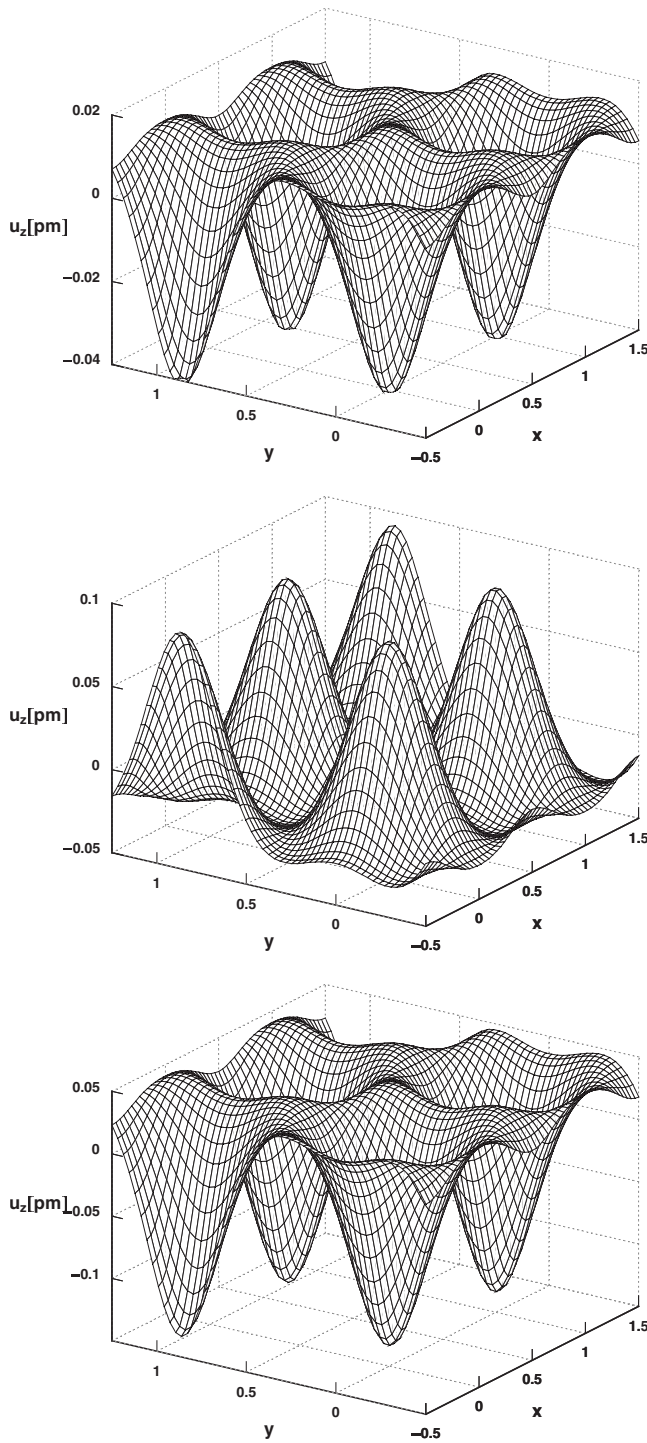


FIG. 2. Surface corrugation $u_z(\mathbf{r})$ of Nb (top) compared to the value neglecting surface dipoles (middle) and only surface dipoles (bottom). The temperatures and the mean magnetic fields are $T=0.95$ and $T_c=9$ K, and $\bar{B}=0.21$ and $B_{c2}(T)=6.4$ mT. The length unit is the vortex distance $a=128$ nm.

planes, i.e., the magnetic field along the c axis. As one can see, the maximum displacement of the surface atom is more than 0.5 \AA , which can be observed by the scanning microscope. Again, neglecting the surface dipole, one arrives at the opposite displacements and while using only the surface dipole, one overestimates the magnitude.

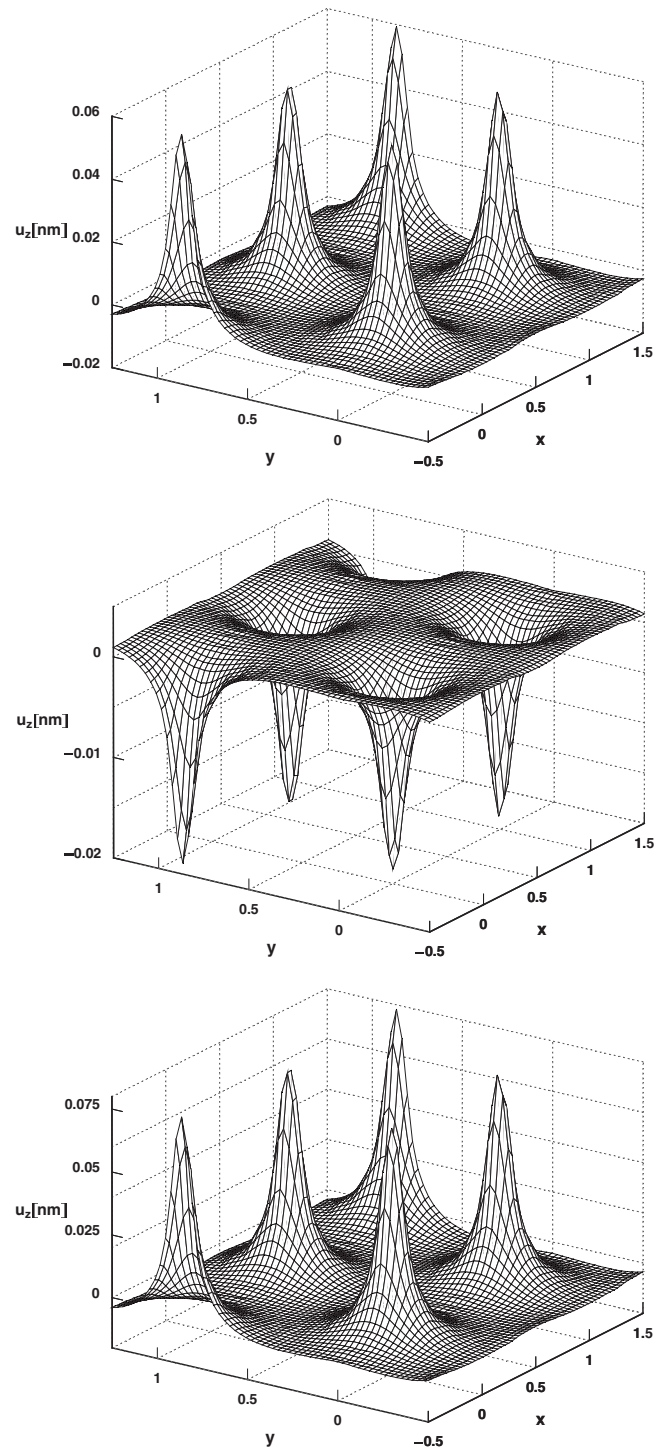


FIG. 3. Surface corrugation $u_z(\mathbf{r})$ of $\text{YBa}_2\text{Cu}_3\text{O}_7$ (top) as compared to the value neglecting surface dipoles (middle) and only surface dipoles (bottom). The temperature and the mean magnetic field are $T=0.67$ and $T_c=60$ K, and $\bar{B}=0.01$ and $B_{c2}(T)=0.6$ T. The length unit is the vortex distance $a=58$ nm.

Perhaps, we should note that the application of the isotropic model to the layered structure of $\text{YBa}_2\text{Cu}_3\text{O}_7$ is not justified. One clearly needs more elastic coefficients to describe the deformation of this highly anisotropic material.²³ The

presented data can thus serve only as an order of magnitude estimate.

VI. CONCLUSIONS

Magnetic field entering a superconductor in the form of vortices induces a corrugation of the surface. In conventional superconductors, the displacement of surface atoms is on the order of 10^{-4} Å, which is too small to be observed by recent experimental tools. In high- T_c superconductors, one can expect amplitudes of $\sim 10^{-1}$ Å, which is in the reach of scanning force microscopes.

Our results for niobium and $\text{YBa}_2\text{Cu}_3\text{O}_7$ show that among the forces that drive the surface corrugation the dominant one is due to the surface dipole. The contribution of the bulk potential to the surface corrugation is opposite to the contri-

bution of the surface; therefore, it reduces the magnitude of the atomic displacement.

Since the deformation of the crystal near the surface differs from the deformation in the bulk, one can expect that the surface terms play an important role in Šimánek contribution to the vortex mass in thin layers. We leave this problem for a future work.

ACKNOWLEDGMENTS

This work was supported by research plans MSM Grants No. 0021620834 and No. AVOZ10100521, by GAČR Grants No. 202/07/0597 and No. 202/08/0326, by GAAV Grant No. 100100712, by PPP project of DAAD, by DFG Priority Program 1157 via Grant No. GE1202/06 and the BMBF, and by European ESF program NES.

-
- ¹E. Šimánek, Phys. Lett. A **154**, 309 (1991).
²J.-M. Duan and E. Šimánek, Phys. Lett. A **190**, 118 (1992).
³E. M. Chudnovsky and A. B. Kuklov, Phys. Rev. Lett. **91**, 067004 (2003).
⁴M. W. Coffey, Phys. Rev. B **49**, 9774 (1994).
⁵H. Ullmaier, R. Zeller, and P. H. Dederichs, Phys. Lett. **44A**, 331 (1973).
⁶V. G. Kogan, L. N. Bulaevskii, P. Miranović, and L. Dobrosavljević-Grujić, Phys. Rev. B **51**, 15344 (1995).
⁷R. Kaschner and P. Ziesche, Phys. Status Solidi B **138**, 65 (1986).
⁸R. Kaschner and P. Ziesche, Phys. Scr. **38**, 414 (1988).
⁹P. Lipavský, K. Morawetz, J. Koláček, E. H. Brandt, and M. Schreiber, Phys. Rev. B **77**, 014506 (2008).
¹⁰L. D. Landau and E. M. Lifshitz, *Elasticity* (Pergamon, Oxford, 1975).
¹¹P. Lipavský, K. Morawetz, J. Koláček, and E. H. Brandt, Phys. Rev. B **76**, 052502 (2007).
¹²H. F. Budd and J. Vannimenus, Phys. Rev. Lett. **31**, 1218 (1973).
¹³A. Kleina and K. F. Wojciechowski, *Metal Surface Electron Physics* (Elsevier Sciences, Oxford, 1996).
¹⁴P. Lipavský, K. Morawetz, J. Koláček, J. J. Mareš, E. H. Brandt, and M. Schreiber, Phys. Rev. B **69**, 024524 (2004).
¹⁵P. Lipavský, J. Koláček, K. Morawetz, and E. H. Brandt, Phys. Rev. B **65**, 144511 (2002).
¹⁶P. Lipavský, J. Koláček, K. Morawetz, E. H. Brandt, and T. J. Yang, *Bernoulli Potential in Superconductors*, Lecture Notes in Physics No. 733 (Springer, Berlin, 2007).
¹⁷P. Lipavský, K. Morawetz, J. Koláček, J. J. Mareš, E. H. Brandt, and M. Schreiber, Phys. Rev. B **71**, 024526 (2005).
¹⁸E. H. Brandt, Phys. Rev. B **71**, 014521 (2005).
¹⁹See physical properties in www.webelements.com
²⁰The pairable charge per Cu atoms is $-0.4335 e$. Figure 2.16 of Plakida (Ref. 24) shows the results of Cava (Ref. 25), according to which the charge transfer $-0.03 e$ from chains to planes per Cu site leads to a decrease in the critical temperature by 30 K. This corresponds to $\frac{\partial \ln T_c}{\partial nn} = -4.82$. From Fig. 3 of Ref. 26 we can see that the specific heat coefficient drops at the same time from 4.4 mJ/gK^2 to 3.0 mJ/gK^2 , which gives $\frac{\partial \ln \gamma}{\partial nn} = -4.13$. This is only a rough estimate since the specific heat data include chains, while we need the change in plane only.
²¹Y. M. Soifer, A. Verdyan, I. Lapsker, and J. Azoulay, Physica C **408**, 846 (2004).
²²N. P. Kobelev, R. K. Nikolaev, N. I. Sidorov, and Y. M. Soifer, Phys. Status Solidi A **127**, 355 (1991).
²³K. Suenaga and G. Oomi, J. Phys. Soc. Jpn. **60**, 1189 (1991).
²⁴N. M. Plakida, *High-Temperature Superconductivity* (Springer-Verlag, Berlin, 1995).
²⁵R. J. Cava, A. W. Hewat, E. A. Hewat, B. Batlogg, M. Marezio, K. M. Rabe, J. J. Krajewski, W. F. Peck, and L. W. Rupp, Physica C **165**, 419 (1990).
²⁶J. W. Loram, K. A. Mirza, J. R. Cooper, and W. Y. Liang, Phys. Rev. Lett. **71**, 1740 (1993).